JOURNAL OF THE ROYAL SOCIETY Interface

CrossMark click for updates

J. R. Soc. Interface (2012) **9**, 2290–2298
doi:10.1098/rsif.2011.0901
Published online 14 March 2012

Spatio-temporal development of the endothelial glycocalyx layer and its mechanical property *in vitro*

Ke Bai and Wen Wang*

Institute for Bioengineering, Queen Mary University of London, Mile End Road, London E1 4NS, UK

The endothelial glycocalyx is a thin layer of polysaccharide matrix on the luminal surface of endothelial cells (ECs), which contains sulphated proteoglycans and glycoproteins. It is a mechanotransducer and functions as an amplifier of the shear stress on ECs. It controls the vessel permeability and mediates the blood–endothelium interaction. This study investigates the spatial distribution and temporal development of the glycocalyx on cultured ECs, and evaluates mechanical properties of the glycocalyx using atomic force microscopy (AFM) nano-indentation. The glycocalyx on human umbilical vein endothelial cells (HUVECs) is observed under a confocal microscope. Manipulation of the glycocalyx is achieved using heparanase or neuraminidase. The Young's modulus of the cell membrane is calculated from the force–distance curve during AFM indentation. Results show that the glycocalyx appears predominantly on the edge of cells in the early days in culture, e.g. up to day 5 after seeding. On day 7, the glycocalyx is also seen in the apical area of the cell membrane. The thickness of the glycocalyx is approximately 300 nm–1 μm. AFM indentation reveals the Young's modulus of the cell membrane decreases from day 3 (2.93 ± 1.16 kPa) to day 14 (0.35 ± 0.15 kPa) and remains unchanged to day 21 (0.33 ± 0.19 kPa). Significant difference in the Young's modulus is also seen between the apical (1.54 ± 0.58 kPa) and the edge (0.69 ± 0.55 kPa) of cells at day 7. By contrast, neuraminidase-treated cells (i.e. without the glycocalyx) have similar values between day 3 (3.18 ± 0.88 kPa), day 14 (2.12 ± 0.78 kPa) and day 21 (2.15 ± 0.48 kPa). The endothelial glycocalyx *in vitro* shows temporal development in the early days in culture. It covers predominantly the edge of cells initially and appears on the apical membrane of cells as time progresses. The Young's modulus of the glycocalyx is deduced from Young's moduli of cell membranes with and without the glycocalyx layer. Our results show the glycocalyx on cultured HUVECs has a Young's modulus of approximately 0.39 kPa.

Keywords: vascular endothelium; the glycocalyx; confocal microscopy; atomic force microscopy nano-indentation; Young's modulus

1. INTRODUCTION

Endothelial cells (ECs) line the entire luminal surface of blood vessels and are in direct contact with the blood. They play vital roles in vascular regulation and blood cell activation and migration during physiological and pathological processes [1,2]. Dysfunction of ECs is a key factor in the initiation and progression of vascular diseases, such as atherosclerosis [3]. At the luminal surface of the endothelium, the glycocalyx exists and forms a brush-like structure of between several hundreds nanometres and a few micrometres in thickness [4,5]. It contains negatively charged molecules such as proteoglycans, glycosaminoglycans (GAGs), glycoprotein and plasma proteins [6,7]. The molecules that make up the glycocalyx are continuously synthesized by and shed from ECs in a dynamic process [8,9]. The endothelial glycocalyx serves a number of functions in the vascular system: (i) permeability control of fluid and solute filtration and absorption across the vessel wall [10–12]; (ii) modification and amplification of the shear stress on ECs by the circulating blood [13,14]; (iii) regulation of interactions between blood cells and vascular ECs [15,16]; in addition, (iv) the glycocalyx functions as a mechanotransducer for the endothelial cytoskeleton [17–22]. It has been reported by several laboratories that manipulation of the glycocalyx, both *in vivo* and *in vitro*, results in the dysfunction of the endothelial mechanotransduction. For example, Thi *et al.* [22,23] reported that following GAGs digestion from HUVECs *in vitro* using heparinase III, effects of the shear stress on the endothelial cytoskeleton was abolished. By contrast, van den Berg *et al.* [24] reported that atherogenic diet mice had much thinner glycocalyx layer than the normal diet ones, making them at higher risk of developing atherosclerosis.

Cell mechanical properties are strongly linked to cell functions, such as cell morphology, adhesion, migration

*Author for correspondence (wen.wang@qmul.ac.uk).

Received 22 December 2011
Accepted 23 February 2012

and signalling [25–27]. Since 1980s, atomic force microscopy (AFM) has been used to investigate properties of biological cells [28,29]. Elastic properties of a number of cell types have been studied using AFM, e.g. Sato *et al.* [30,31] estimated the elasticity of HUVECs and reported the Young's modulus changes with time during the early stage of cell culture. Kataoka *et al.* [32] reported the elastic modulus of cultured HUVECs was 3.0–6.7 kPa in their AFM study. The Young's modulus of other cell types has also been studied. They include chondrocytes (0.6 kPa) [33], 3T3 fibroblasts (3–12 kPa) [34] and human chondrosarcoma cell (2 kPa) [35] to list a few. Mechanical properties of the glycocalyx have not been studied until very recently. Oberleithner *et al.* [36] reported the stiffness of the glycocalyx on cultured bovine aortic endothelial cells (BAECs) to be 0.25 pN nm^{-1}. O'Callaghan *et al.* [37] measured the Young's modulus of the glycocalyx on bovine lung microvascular endothelial cells (BLMVECs) and reported a value of 0.26 ± 0.03 kPa. However, to our knowledge, there has been no experimental study on the spatial variation or the temporal development of the glycocalyx layer on cell membrane. Giving its strategic location as the interface between the blood and the endothelium, the glycocalyx mediates flow-induced shear stress on ECs. A sound knowledge of the mechanical properties of the glycocalyx layer is essential for us to understand its many biological functions.

In the current study, we observe the spatial distribution of the endothelial glycocalyx layer using laser-scanning confocal microscopy. Cells after different days in culture are studied to evaluate the temporal development of the glycocalyx layer. Comparisons are made between the controls and enzyme-treated groups. In addition, we have investigated mechanical properties of the glycocalyx layer using AFM nanoindentation. The Young's modulus of the glycocalyx is calculated by analysing testing results on the HUVEC cell membrane with and without the glycocalyx layer. The study gives quantitative insights into the spatial distribution and temporal development of the endothelial glycocalyx layer *in vitro*, and improves our understanding of the glycocalyx recovery mechanism which is of fundamental importance in vascular pathophysiology.

2. MATERIAL AND METHODS

2.1. Cell culture and cell proliferation

HUVECs (primary pooled) are purchased from Lonza (Lonza Cologne AG, Germany). They are thawed and cultured in the M199 medium (Gibco) in collagen type I-coated flasks (5 μg ml^{-1}) at 37°C and 5 per cent CO_2. The culture medium contains 10 per cent foetal bovine serum, EC growth factor-β (1 ng ml^{-1}), EC growth supplement from bovine neural extract (3 μg ml^{-1}), thymidine (1.25 μg ml^{-1}), heparin (10 μg ml^{-1}), 100 U ml^{-1} penicillin, 100 mg ml^{-1} streptomycin (all supplements are from Sigma Aldrich). The medium is changed every 2 days. After reaching 80 per cent confluence, HUVECs are treated with 0.25 per cent trypsin containing 0.02 per cent ethylenediaminetetraacetic acid (EDTA; Sigma Aldrich) and cells are split and seeded on collagen type I-coated glass slide. Following different periods of culture (in this study, days 1, 3, 7, 14 and 21 are investigated), cells are either immunofluorescently labelled for confocal observations or ready for AFM probing.

2.2. Ex vivo preparation of mouse thoracic aortas

All animal experiments are performed according to protocols approved by the institutional committee for use and care of laboratory animals. C57BL/6 mice (two to four months old, 20–30 g body weight) are anaesthetized and thoracic aortas are harvested.

2.3. Enzyme treatment with either neuraminidase or heparinase III

Neuraminidase from *Clostridium perfringens* (Sigma Aldrich) is used in the study. It cleaves N-acetyl neuraminic acid residues of glycoproteins and targets specifically the sialic acid component of the endothelial glycocalyx. Cultured HUVECs or segments of mouse thoracic aorta are treated with neuraminidase according to the protocol by Baker *et al.* [38]. Serum-free M199 medium is used to wash the sample gently twice before it is incubated with 1 U ml^{-1} neuraminidase for 10 min at 37°C. The control group remains in the HUVECs culture medium.

Heparinase type III (Sigma Aldrich) cleaves heparan sulphate GAGs. HUVECs or aorta segments are gently washed twice using the serum-free M199 medium and incubated with 0.5 U ml^{-1} heparinase III for 30 min at 37°C. The control group is kept in the HUVEC culture medium.

2.4. Immunocytochemistry and immunofluorescence imaging

Wheat germ agglutinin (WGA-FITC) is used to bind to N-acetly-D-glucosamine and sialic acid component of the glycocalyx [38,39]. Heparan sulphates are stained by heparan sulphate antibody FITC (HepSS-1, US biological) [22]. The endothelial cytoplasm is stained by Cell Tracker Red CMTPX (Invitrogen). EC tight junctions are stained using CD144 (Santa Cruz) and cell nucleus are stained using DAPI or Hoechst 33342 (Sigma Aldrich).

The aortas are cut open along the axis of the vessel and unfolded onto a Petri dish with the luminal surfaces on the top. The aorta segments are fixed by 4 per cent paraformaldehyde for 10 min at room temperature, followed by 20 per cent rabbit serum blocking for 30 min at 37°C. After that, HepSS-1 (figure 1) or WGA-FITC (figure 2) and CD144 (in both figures 1 and 2) are applied on the segment for 1 h at 37°C. DAPI is then applied for 10 min at 37°C. Segments are washed three times by serum-free M199 after staining and kept in 10 per cent serum culture medium, ready for confocal microscopy (Leica Microsystems, Wetzlar, Germany).

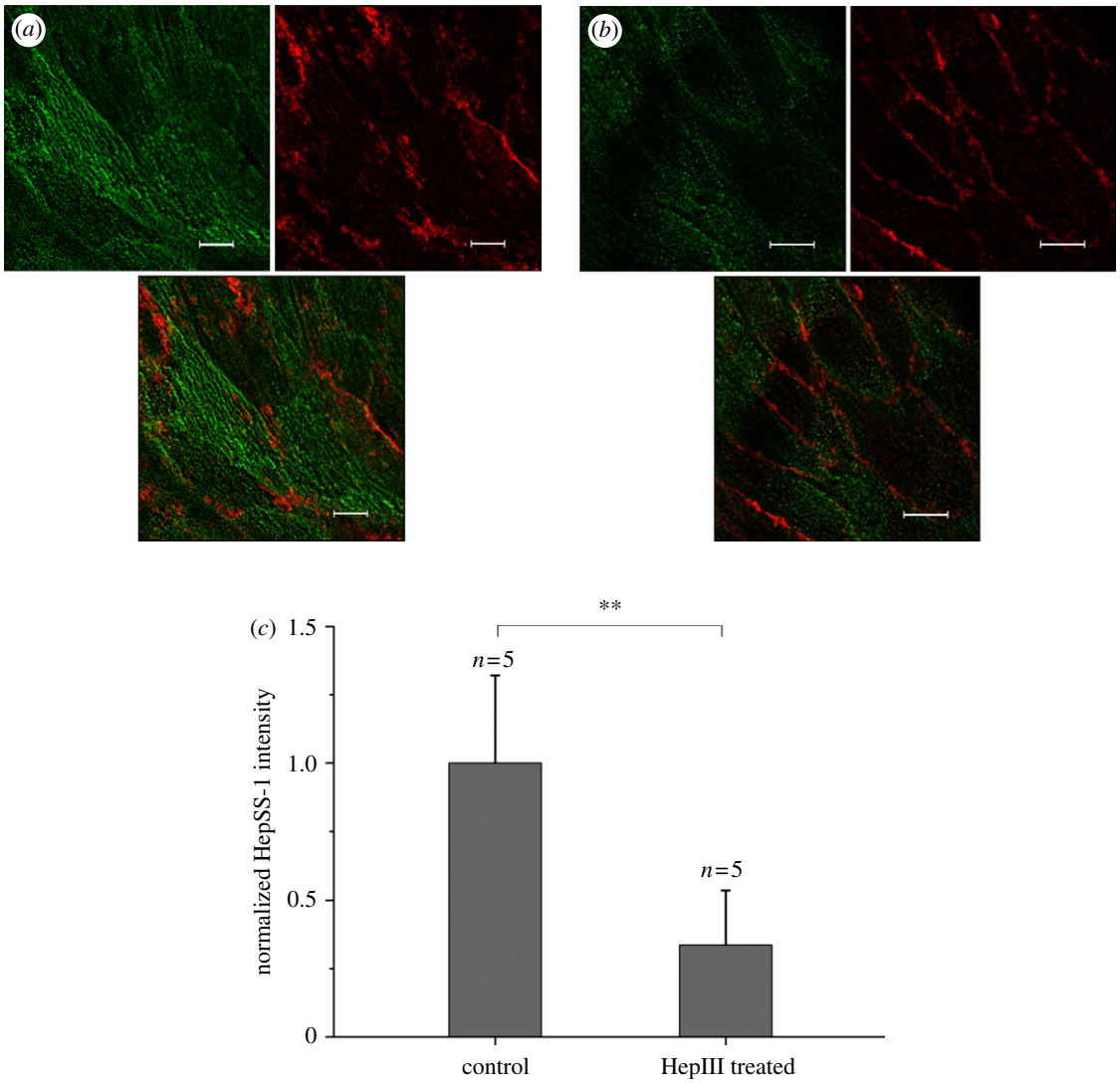

Figure 1. *Ex vivo* HepSS-I (green) and CD144 (red) staining of the mouse thoracic aortic endothelium. (*a*) Control, (*b*) after HepIII treatment, (*c*) change in the green dye intensity following enzyme perfusion of the aorta. (*a*,*b*) Scale bars, 10 µm.

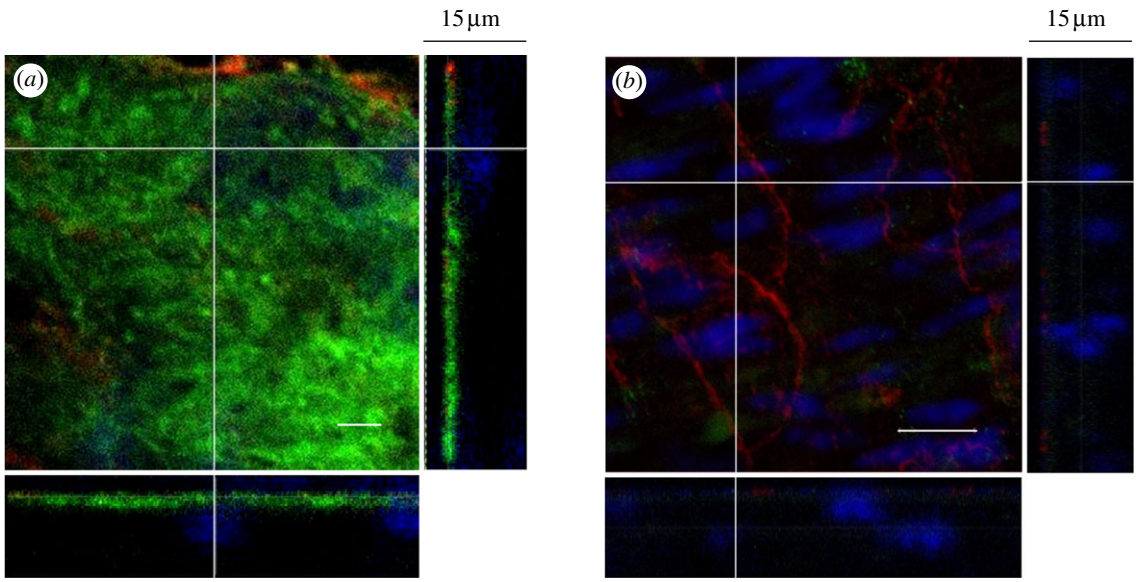

Figure 2. Three-dimensional confocal images of the glycocalyx layer on freshly harvest and unfixed mouse thoracic aorta. The main panel shows the enface image at a given *z*-depth. The bottom and side panels show the *x*–*z* and *y*–*z* cross-sectional images, respectively. Scale bar, 10 µm, in the main panel. (*a*) Control, (*b*) after neuraminidase perfusion of the aorta.

Cultured HUVECs are briefly washed using the serum-free M199. WGA-FITC and Cell Tracker Red are applied to live cells for 15 min at 37°C before Hoechst 33342 is applied for 5 min. Live cells are washed and immersed in culture medium (with 10% serum) immediately after staining. They are kept in the serum-containing culture medium during confocal observation.

Intensities of the green (heparan sulphate) and red (CD144) dyes are analysed using the software Image J (National Institutes of Health, USA).

2.5. Atomic force microscopy measurements

HUVECs are cultured in collagen-coated cover slips ($d = 13$ mm). The cover slip is placed on a microscopic liquid sample stage. Measurements are carried out using an AFM in our laboratory (NT-MDT Ntegra System). The cantilever (Olympus, OMCL-RC800PSA-1) has a pyramidal-shaped tip, and the end of the tip is hemispherical shaped with a radius of 20 nm (shown in figure 4*b*). The surface of the cell membrane is divided into three regions as shown in figure 4*d*: apical (i.e. above the cell nucleus), middle and edge, with the middle and the edge regions of approximately equal sizes. The height and phase images of HUVECs are taken under tapping mode [40]. Indentation tests are carried out under contact mode on samples within 1 h after they are removed from the incubator. During AFM probing, samples are kept in the culture medium.

2.6. Analysis of force–distance curves

The Hertz model for indentation of a homogeneous soft sample by a stiff cone was used to analyse the force–distance curve [31,41]

$$F = \delta^2 \frac{2}{\pi} \frac{E}{(1-\nu^2)} \tan\alpha,$$

where F is the applied loading force, δ is the indentation distance, ν is the Poisson ratio of the tissue sample and is assumed to be 0.5 as cells are considered to be incompressible, α is the half opening angle of the tip of the AFM cantilever and E is the Young's modulus.

3. RESULTS

3.1. Ex vivo observation of the endothelial glycocalyx in fixed samples

Mouse thoracic aortas are cut open along the axis of the vessel and pinned onto a Petri dish with the endothelium facing upwards, as shown in figure 1*a,b*. The green-strained heparan sulphate-containing layer, seeing in (*a*), becomes much less expressed after HepIII treatment, as shown in (*b*). When we compare the intensity of the green dye in heparinase III-treated groups to that in control groups, as shown in figure 1*c*, we observe a statistically very significant decrease ($p < 0.01$) following the enzyme perfusion of the aortic endothelium. The *ex vivo* results show that the staining and enzyme treatment protocols for the glycocalyx as well as the confocal image system work properly in our study.

3.2. Three-dimensional-reconstructed images of the glycocalyx in unfixed ex vivo samples

In order to estimate the depth of the glycocalyx layer in blood vessels *ex vivo*, we have used freshly harvest and unfixed mouse thoracic aorta in figure 2. Different to experiments in figure 1, WGA-FITC is used to bind to the heparan sulphate and hyaluronic acid of the unfixed tissue samples. Three-dimensional confocal images are taken at a series of depths (at $\Delta z = 200$ nm interval along the z-axis). The main enface panel shows the fluorescent image in the x–y cross section at a given z-location (rather than stack images). The two smaller panels reveal the structure of the glycocalyx layer along the x–z (bottom panel) and y–z cross sections (side panel) as indicated by dashed lines in the enface image. The intact glycocalyx layer, seen in figure 2*a*, has a similar expression to that in figure 1*a*. The green-stained layer is approximately 1–2 μm in depth and is confined to the surface of the endothelium, as indicated by the red-stained endothelial-specific tight junctions. For neuraminidase-treated samples, shown in figure 2*b*, there is little green-stained layer in the enface image. Here, nuclei of ECs and smooth muscle cells are stained blue. The bottom and side panels in figure 2*b* reveal largely green free cross sections in the x–z and y–z planes. These *ex vivo* results agree with previous findings where the thickness of endothelial glycocalyx layer was estimated to be between several hundred nanometres to several micrometres [24,42,43].

3.3. The glycocalyx on unfixed human umbilical vein endothelial cells in vitro: temporal development and spatial distribution

Live HUVEC monolayer on cover slips is stained by WGA-FITC for the extracellular component of heparan sulphate and HA, Cell Tracker Red CMTPX for the endothelial cytoplasm and Hoechst 33342 for cell nuclei. Cells are unfixed to limit structural alternations to the cell membrane layer and are observed at different days, i.e. 1, 3, 5, 7, 14 and 21, of cell culture (figure 3*a*). Three-dimensional confocal images are taken from the top of the cell to the glass slide. Heparan sulphate and HA components of the glycocalyx layer are observed on the endothelial membrane. Initially during cell culture, e.g. the end of day 1, the green dye appears only at the edge of cells. Similar patterns are seen in day 3 and day 5, although there is more distribution of the green dye along the edge of cells. As time progresses, by the end of day 7, the green dye appears not only near the edge of cells, but also towards the apical area, although it is still quite patchy on the membrane above the endothelial nucleus. By the end of day 14, the green dye can be seen over the entire cell membrane. From the z-section images (shown as the bottom and side panels), the thickness of the glycocalyx layer on HUVECs *in vitro* is between 300 nm and 1 μm. This layer is thinner compared with the one on the *ex vivo* sample, but after 14 days in culture, it covers the entire surface of the cell membrane, forming a continuous layer like that in figure 2*a*. By contrast, neuraminidase-treated HUVECs, shown in figure 3*b*,

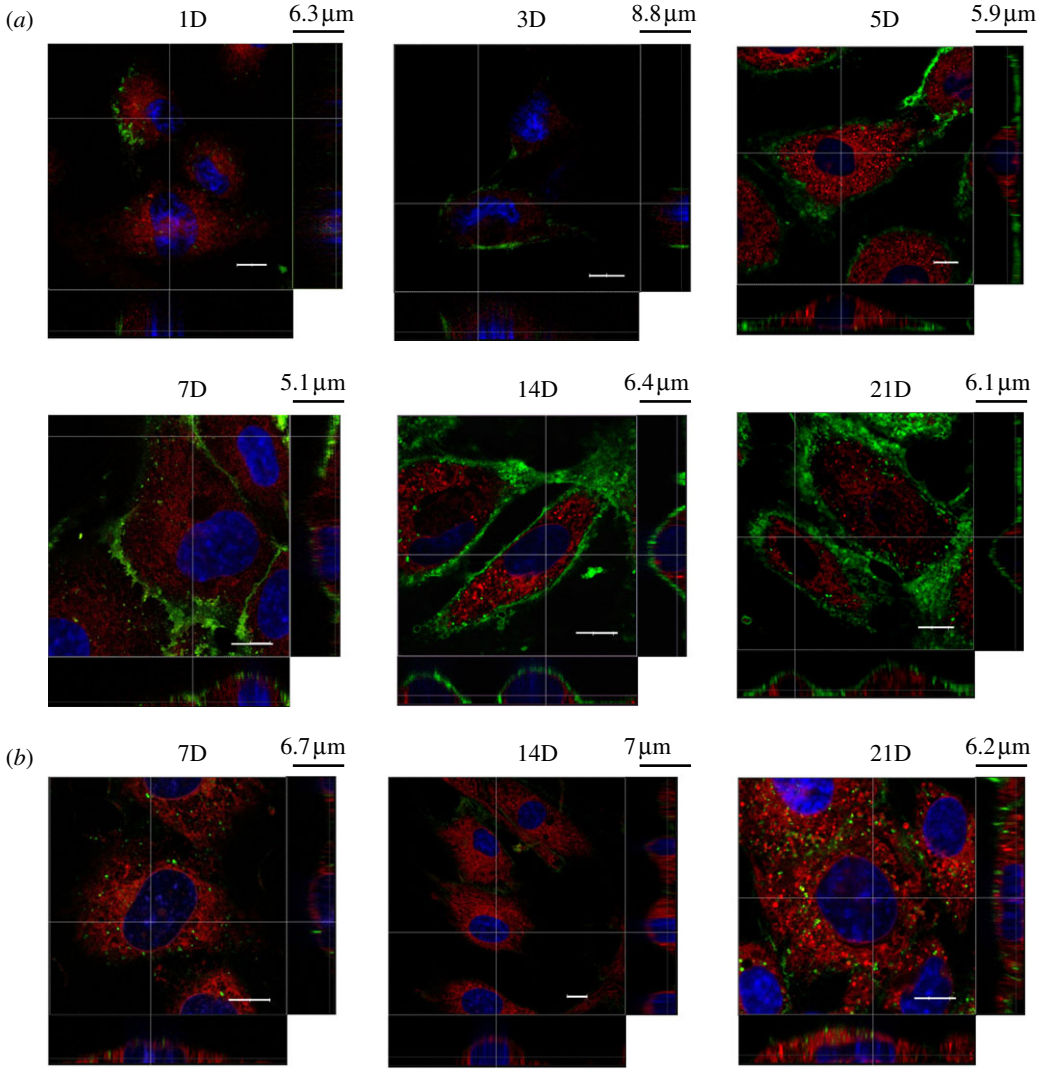

Figure 3. Spatial distribution of the glycocalyx layer on live HUVECs *in vitro* and its temporal development from day 1 to day 21. The main panel shows the enface image at a given z-depth. The bottom and side panels show the x–z and y–z cross-sectional images, respectively. Scale bar, 10 µm, in the main panel. (*a*) Control, (*b*) after neuraminidase treatment.

at day 7, 14 and 21 do not present a layer of the green dye after they are stained by WGA, indicating that the enzyme has cleaved away most of the glycocalyx from the cell membrane.

3.4. The mechanical properties of the glycocalyx using atomic force microscopy indentation

In order to study the mechanical properties of the glycocalyx layer, AFM has been applied to investigate the force–displacement relationship during nano-indentation tests on HUVEC membrane. By comparing the Young's modulus of ECs at different days of cell culture, before and after enzyme treatment, we hope to gain further evidence on the spatial distribution of the glycocalyx on cell membranes and its temporal development *in vitro*.

Figure 4*a* is a schematic of the AFM cantilever scanning through the HUVEC monolayer. The cantilever tip reflects a laser beam, and the oscillation of the tip is recorded by a position-sensitive detector. In our study, a rectangular cantilever with a pyramid-shaped tip is used for both topographic imaging and indentation of cells. The cantilever, shown in figure 4*b*, is 100 µm in length and 20 µm in width, with a known spring constant (0.38 N m^{-1}). The tip is pyramid-shaped with a base length of 5.2 µm and a height of 2.9 µm. The half opening angle is approximately 41°. The end of the tip has a semi-spherical shape with a radius of approximately 20 nm. Both the height and phase images are taken simultaneously in the study to gain information of the cell surface. In figure 4*c*, the brightness of the image indicates the height of the cell surface, whereas in figure 4*d*, the phase image provides contrast of the change in height and gives a better indication of location of the edge of cells. In later studies, we divide the cell surface into three regions: the 'apical' region is the area above the endothelium nucleus, and the rest area is divided equally into the 'middle' and the 'edge' regions. This enables spatial distinction of the cell membrane surface.

Nano-indentation tests are performed on different locations of the cell surface using the contact mode.

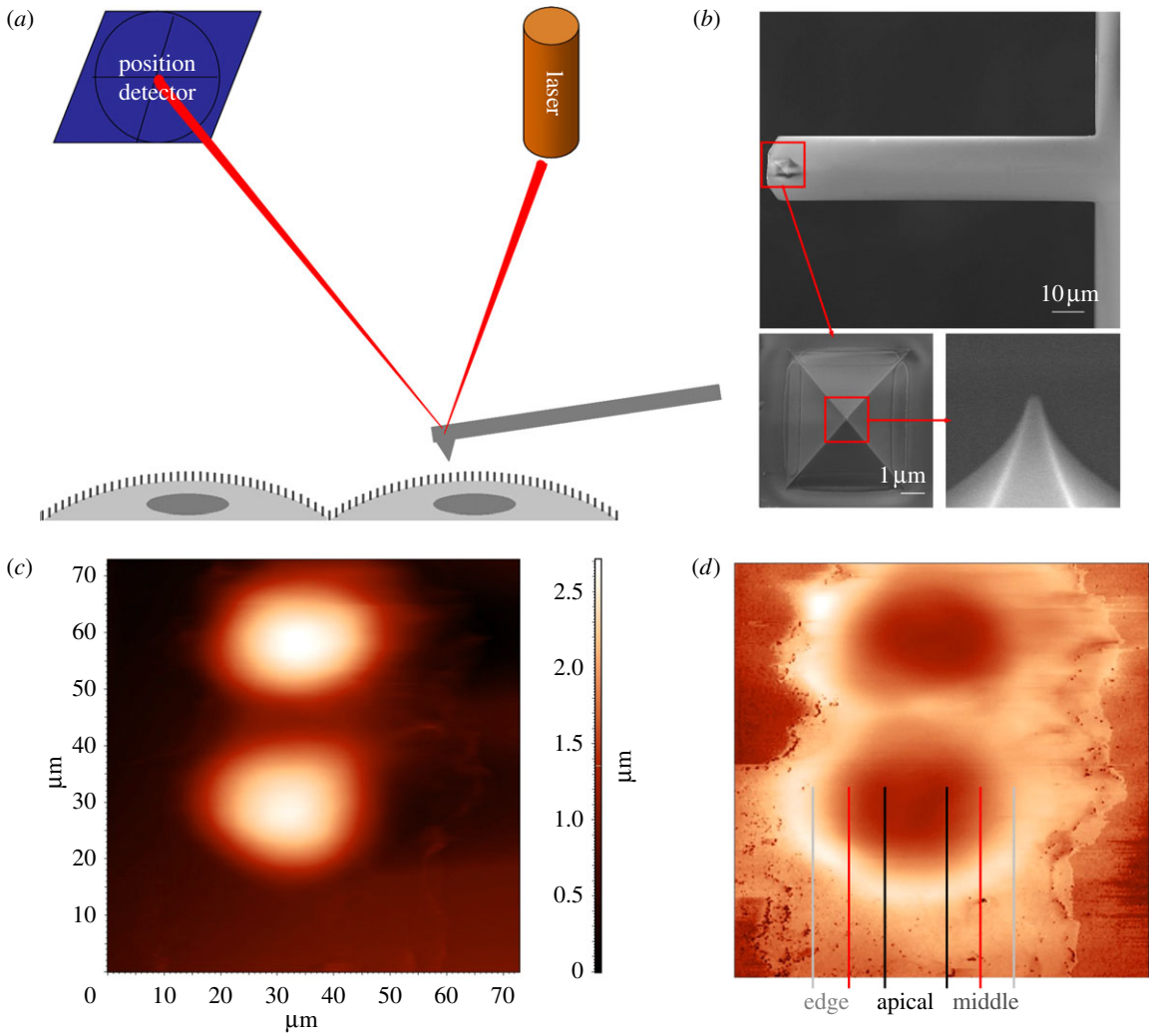

Figure 4. (*a*) Schematics of AFM probing of HUVECs *in vitro*, (*b*) rectangular cantilever, pyramidal-shaped tip (enlarged panel), the end of the tip is semi-spherical (further enlarged panel), (*c*) height image of HUVECs, (*d*) phase image of HUVECs. (Online version in colour.)

The Young's modulus of the cell membrane is calculated from the force–distance curve over the initial 200 nm of indentation. During an indentation, the cantilever also bends. In order to measure the true indentation distance of the AFM tip against the cell membrane, the movement of the tip owing to bending of the cantilever needs to be subtracted from the total distance. This is achieved by a calibration test of the cantilever indenting against the glass slide, where the bending distance of the cantilever under known values of the indentation force is measured. In figure 5, Young's moduli of the cell membrane at three different locations on the cell membrane are presented. HUVECs at the end of day 3, 7, 14 and 21 in culture are used. Comparisons are made between cells with and without the glycocalyx layer, i.e. between control groups and corresponding groups following neuraminidase treatment.

When we compare control groups in days 3, 7, 14 and 21 only, it is seen that the Young's modulus of the cell membrane decreases with time, from approximately 2.93 kPa (± 1.16 kPa, $n = 27$) at day 3 to 1.20 kPa (± 0.51 kPa, $n = 26$) at day 7, further decreases to 0.35 kPa (± 0.15 kPa, $n = 28$) at day 14, then remains unchanged at 0.33 kPa (± 0.19 kPa, $n = 27$) to day 21. This reflects the development of the glycocalyx layer, which is a more flexible structure, on the cell membrane and results in progressively reduced values in the Young's modulus as the layer develops with time. After day 14, the glycocalyx layer is well developed and the value remains unchanged. In comparison, when we look at neuraminidase-treated groups, the Young's modulus is greater in all cases in comparison with their respective control groups. These increases are statistically significant ($p < 0.05$, denoted by *) except for day 3, and are statistically very significant ($p < 0.01$, denoted by **) for day 14 and day 21. A close look at the control group at day 7 reveals that the difference in Young's modulus between the apical (1.54 ± 0.58 kPa, $n = 9$) and the edge (0.69 ± 0.55 kPa, $n = 8$) of the cell is significantly different ($p = 0.012$). This is consistent with earlier results from the confocal microscopy, where the glycocalyx layer at day 7 is mainly around the edge of cells and less well developed in the apical region above the cell nucleus. If we compare neuraminidase-treated groups at day 14 and day 21 to their control groups, the stiffness of HUVEC cell membrane increases by more than sixfolds, i.e. from

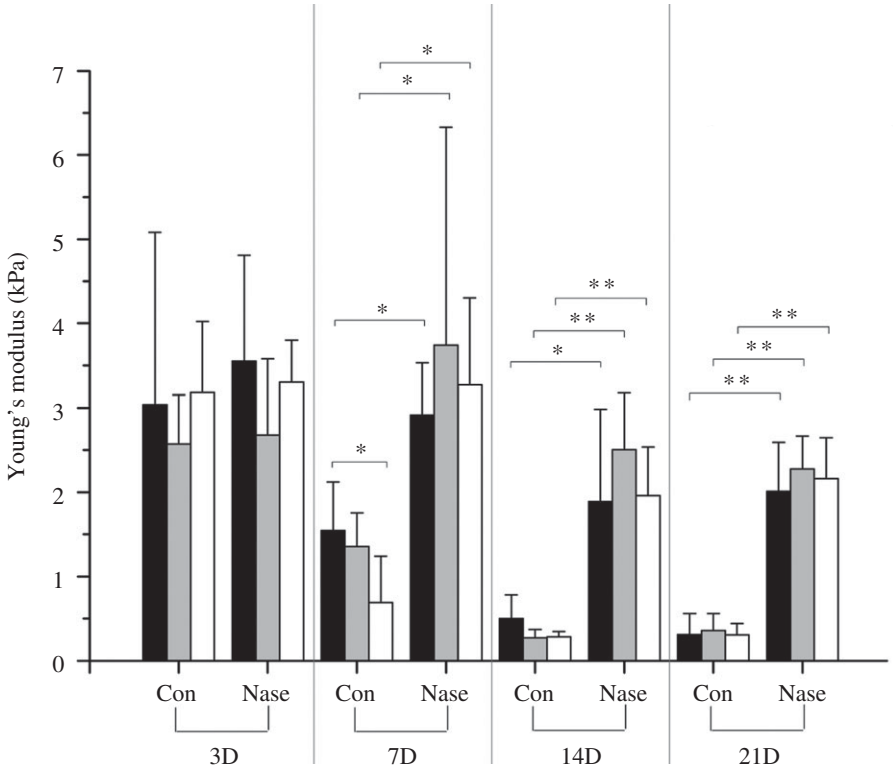

Figure 5. The Young's modulus of the HUVEC membrane *in vitro*. HUVECs cultured for 3, 7, 14 and 21 days are tested using AFM indentation. Comparisons are made between different locations (i.e. apical, middle and edge) on the cell membrane, as well as between the control groups (Con) and neuraminidase-treated groups (Nase) at different days. Black bars, apical; grey bars, middle; white bars, edge.

approximately 0.34–2.13 kPa, when the glycocalyx layer is cleaved away.

4. DISCUSSION

Previous studies have reported a wide range of values on the thickness of the glycocalyx layer. This is partly due to different species and different types of blood vessels used in experiments, and partly due to different preparation techniques employed. Most notably, the dehydration and fixation process for conventional electron microscopy would likely collapse all but the protein cores of proteoglycans and water crystals might form [44]. For example, Vink's group reported a 0.2–0.5 μm hairy structure of the glycocalyx layer in ventricular myocardial capillaries of the rat heart using electron microscopy [42]. On the other hand, Megens *et al.* [39], based on their three-dimensional reconstruction images using two-photon laser-scanning microscopy, reported that in mice mesenteric arteries, the glycocalyx layer was approximately 4.5 μm and covered two-thirds of the entire endothelial surface area. The debate on differences between the endothelial glycocalyx *in vivo* and *in vitro* has involved not only on the thickness of the glycocalyx, but also on the functionality of the *in vitro* glycocalyx layer. Chappell *et al.* [43] reported that HUVECs possessed the glycocalyx structure only in their *ex vivo* samples and not on cultured cells. In a more recent paper by Ebong *et al.* [45], the glycocalyx layer on cultured bovine aortic ECs and rat fat pad ECs have been observed using rapid freezing/freeze substitution transmission electron microscopy. Based on this unconventional approach, the endothelial glycocalyx layer was estimated to be approximately 5–10 μm, i.e. approximately 100-fold thicker than what was observed on conventionally preserved ECs. Their observation of stained heparan sulphates using confocal microscopy showed similar thickness (i.e. approximately 1.4 μm) of the glycocalyx layer as reported in the current study.

In *ex vivo* confocal images, CD144 staining shows a notable difference between the control group and enzyme treatment group. This may be caused by the glycocalyx layer in the control group restricting the access of CD144 dye to cell tight junctions. In enzyme-treated groups, where the glycocalyx layer has been largely diminished, tight junctions are exposed and directly accessible by CD144. Images there reveal a typical continuous and cobblestone pattern for the EC junctions.

Our *in vitro* results using confocal microscopy show the development of the endothelial glycocalyx over time. The growth appears to initiate from the edge of cells and takes up to two weeks to cover the apical region of the cell membrane (i.e. region above the nucleus). The mechanism underlining this spatial distribution and temporal change needs further investigation, but it seems functionally beneficial as the glycocalyx layer covers the intercellular gaps for the endothelium to fulfil its role as a selective semi-permeable membrane for the circulating blood. Our three-dimensional reconstructed images, although limited by the confocal

resolution in the z-direction, indicate that the thickness of the glycocalyx layer is approximately 1 μm. This finding agrees reasonably well with previous studies.

Another novelty of the study is on our AFM probing of the mechanical property of the endothelial glycocalyx layer. Indentation of the cell membrane of the initial 200 nm (after bending of the cantilever is deducted) enables us to estimate the Young's modulus of the glycocalyx layer by comparing the change in the cell membrane Young's modulus with and without the glycocalyx. We can simplify the flexible glycocalyx layer on a deformable cell membrane to a two springs in series system. In such a system, the overall spring constant of the system k, can be expressed as

$$k = \frac{k_1 k_2}{k_1 + k_2},$$

where k_1 and k_2 are spring constants of the two individual ones, respectively. Our results suggest that the cell membrane Young's modulus without the glycocalyx layer is approximately 2.13 kPa (average of day 14 and 21), and with the glycocalyx layer, the overall Young's modulus is approximately 0.34 kPa (average of day 14 and 21 control groups). This leads to the Young's modulus of the glycocalyx layer alone to be approximately 0.39 kPa.

AFM indentation of HUVECs at day 7 (the control group) shows a statistically significant difference in the Young's modulus between the edge and apical regions of the cell surface. This difference indicates an uneven spatial development of the glycocalyx on the cell membrane. As time progresses, e.g. at day 14 and day 21, the difference in the Young's modulus at different locations on the cell surface becomes very small. This is consistent to our confocal microscopy results, where the development of the glycocalyx layer is initially around the edge of the cell, then spreads out to cover the apical area above the nucleus.

One of the limitations of the study is the spatial resolution (approx. 200 nm) of the confocal images. This is largely owing to the diffraction limit of the optical system used. We are currently working on a super fine-resolution confocal system, which has the potential to observe the glycocalyx layer in finer detail, but the dense structure of the glycocalyx as well as the dynamic composition of glycans in this layer may present additional challenges for the super fine-resolution optical system to work. Another limitation of the study is the staining of hyaluronan and heparan sulphate components of the glycocalyx layer. They are part of the glycocalyx constituents but may not represent the full depth of the glycocalyx layer. Despite these limitations, the current study demonstrates the spatial distribution and temporal development of the glycocalyx layer on cell surfaces *in vitro*. It provides the first direct measurement of the mechanical property of the glycocalyx layer using an AFM nano-indentation.

W.W. thanks the Royal Academy of Engineering for a Global Research Fellowship that supports his secondment at Harvard University. K.B. is funded by a College PhD studentship from Queen Mary University of London. The project was supported in part by a MRC/EPSRC Discipline Bridging Initiative grant G0502256-77947. Authors thank Dr Asa Barber for his help on studies using AFM.

REFERENCES

1 Middleton, J., Neil, S., Wintle, J., Clark-Lewis, I., Moore, H., Lam, C., Auer, M., Hub, E. & Rot, A. 1997 Transcytosis and surface presentation of IL-8 by venular endothelial cells. *Cell* **91**, 385–395. (doi:10.1016/S0092-8674(00)80422-5)

2 Cai, H. & Harrison, D. G. 2000 Endothelial dysfunction in cardiovascular diseases: the role of oxidant stress. *Circ. Res.* **87**, 840–844. (doi:10.1161/01.RES.87.10.840)

3 Davignon, J. & Ganz, P. 2004 Atherosclerosis: evolving vascular biology and clinical implications. *Circulation* **109**, III-27–III-32. (doi:10.1161/01.CIR.0000131515.03336.f8)

4 Squire, J. M., Chew, M., Nneji, G., Neal, C., Barry, J. & Michel, C. 2001 Quasi-periodic substructure in the microvessel endothelial glycocalyx: a possible explanation for molecular filtering? *J. Struct. Biol.* **136**, 239–255. (doi:10.1006/jsbi.2002.4441)

5 Luft, J. H. 1966 Fine structure of capillary and endocapillary layer as revealed by ruthenium red. *Federation Proc.* **25**, 1773–1783.

6 Oohira, A., Wight, T. N. & Bornstein, P. 1983 Sulfated proteoglycans synthesized by vascular endothelial cells in culture. *J. Biol. Chem.* **258**, 2014–2021.

7 Jackson, R. L., Busch, S. J. & Cardin, A. D. 1991 Glycosaminoglycans: molecular properties, protein interactions, and role in physiological processes. *Physiol. Rev.* **71**, 481–539.

8 Lipowsky, H. H. 2005 Microvascular rheology and hemodynamics. *Microcirculation* **12**, 5–15. (doi:10.1080/10739680590894966)

9 Gouverneur, M., Van Den Berg, B., Nieuwdorp, M., Stroes, E. & Vink, H. 2006 Vasculoprotective properties of the endothelial glycocalyx: effects of fluid shear stress. *J. Intern. Med.* **259**, 393–400. (doi:10.1111/j.1365-2796.2006.01625.x)

10 Levick, J. R. & Michel, C. C. 2010 Microvascular fluid exchange and the revised starling principle. *Cardiovasc. Res.* **87**, 198–210. (doi:10.1093/cvr/cvq062)

11 Michel, C. C. & Kendall, S. 1997 Differing effects of histamine and serotonin on microvascular permeability in anaesthetized rats. *J. Physiol.* **501**, 657–662. (doi:10.1111/j.1469-7793.1997.657bm.x)

12 Weinbaum, S. 1998 Whitaker distinguished lecture: models to solve mysteries in biomechanics at the cellular level; a new view of fiber matrix layers. *Ann. Biomed. Eng.* **26**, 627–643. (doi:10.1114/1.134)

13 Wang, W. & Parker, K. H. 1995 The effect of deformable porous surface layers on the motion of a sphere in a narrow cylindrical tube. *J. Fluid Mech.* **283**, 287–295. (doi:10.1017/S0022112095002321)

14 Mochizuki, S., Vink, H., Hiramatsu, O., Kajita, T., Shigeto, F., Spaan, J. A. E. & Kajiya, F. 2003 Role of hyaluronic acid glycosaminoglycans in shear-induced endothelium-derived nitric oxide release. *Am. J. Physiol. Heart Circ. Physiol.* **285**, H722–H726. (doi:10.1152/ajpheart.00691.2002)

15 Damiano, E. R. 1998 The effect of the endothelial-cell glycocalyx on the motion of red blood cells through capillaries. *Microvasc. Res.* **55**, 77–91. (doi:10.1006/mvre.1997.2052)

16 Zhao, Y., Chien, S. & Weinbaum, S. 2001 Dynamic contact forces on leukocyte microvilli and their penetration

of the endothelial glycocalyx. *Biophys. J.* **80**, 1124–1140. (doi:10.1016/S0006-3495(01)76090-0)
17 Damiano, E. R. & Stace, T. M. 2002 A mechano-electrochemical model of radial deformation of the capillary glycocalyx. *Biophys. J.* **82**, 1153–1175. (doi:10.1016/S0006-3495(02)75474-X)
18 Florian, J. A., Kosky, J. R., Alinslie, K., Pang, Z., Dull, R. O. & Tarbell, J. M. 2003 Heparan sulfate proteoglycan is a mechanosensor on endothelial cells. *Circ. Res.* **93**, e136–e142. (doi:10.1161/01.RES.0000101744.47866.D5)
19 Gouverneur, M., Spaan, J. A., Pannekoek, H., Fontijn, R. D. & Vink, H. 2006 Fluid shear stress stimulates incorporation of hyaluronan into endothelial cell glycocalyx. *Am. J. Physiol. Heart Circ. Physiol.* **290**, H458–H462. (doi:10.1152/ajpheart.00592.2005)
20 Secomb, T. W., Hsu, R. & Pries, A. R. 2001 Effect of the endothelial surface layer on transmission of fluid shear stress to endothelial cells. *Biorheology* **38**, 143–150.
21 Tarbell, J., Weinbaum, S. & Kamm, R. 2005 Cellular fluid mechanics and mechanotransduction. *Ann. Biomed. Eng.* **33**, 1719–1723. (doi:10.1007/s10439-005-8775-z)
22 Thi, M. M., Tarbell, J. M., Weinbaum, S. & Spray, D. C. 2004 The role of the glycocalyx in reorganization of the actin cytoskeleton under fluid shear stress: a 'bumper-car' model. *Proc. Natl Acad. Sci. USA* **101**, 16 483–16 488.
23 Yao, Y., Rabodzey, A. & Dewey Jr, C. F. 2007 Glycocalyx modulates the motility and proliferative response of vascular endothelium to fluid shear stress. *Am. J. Physiol. Heart Circ. Physiol.* **293**, H1023–H1030. (doi:10.1152/ajpheart.00162.2007)
24 van den Berg, B. M., Spaan, J. A. E., Rolf, T. M. & Vink, H. 2006 Atherogenic region and diet diminish glycocalyx dimension and increase intima-to-media ratios at murine carotid artery bifurcation. *Am. J. Physiol. Heart Circ. Physiol.* **290**, H915–H920. (doi:10.1152/ajpheart.00051.2005)
25 Guck, J. *et al.* 2005 Optical deformability as an inherent cell marker for testing malignant transformation and metastatic competence. *Biophys. J.* **88**, 3689–3698. (doi:10.1529/biophysj.104.045476)
26 Yamazaki, D., Kurisu, S. & Takenawa, T. 2005 Regulation of cancer cell motility through actin reorganization. *Cancer Sci.* **96**, 379–386. (doi:10.1111/j.1349-7006.2005.00062.x)
27 Sheetz, M. P. 2006 Cellular plasma membrane domains. *Mol. Membr. Biol.* **12**, 89–91. (doi:10.3109/09687689509038501)
28 Drake, B., Prater, C. B., Weisenhorn, A. L., Gould, S. A., Albrecht, T. R., Quate, C. F., Cannell, D. S., Hansma, H. G. & Hansma, P. K. 1989 Imaging crystals, polymers, and processes in water with the atomic force microscope. *Science* 243, 1586–1589. (doi:10.1126/science.2928794)
29 Henderson, E. 1994 Imaging of living cells by atomic force microscopy. *Progr. Surf. Sci.* **46**, 39–60. (doi:10.1016/0079-6816(94)90006-X)
30 Sato, H., Katano, M., Takigawa, T. & Masuda, T. 2001 Estimation for the elasticity of vascular endothelial cells on the basis of atomic force microscopy and Young's modulus of gelatin gels. *Polym. Bull.* **47**, 375–381. (doi:10.1007/s289-001-8195-z)
31 Sato, H., Kataoka, N., Kajiya, F., Katano, M., Takigawa, T. & Masuda, T. 2004 Kinetic study on the elastic change of vascular endothelial cells on collagen matrices by atomic force microscopy. *Colloids Surf. B Biointerfaces* **34**, 141–146. (doi:10.1016/j.colsurfb.2003.12.013)
32 Kataoka, N., Iwaki, K., Hashimoto, K., Mochizuki, S., Ogasawara, Y., Sato, M., Tsujioka, K. & Kajiya, F. 2002 Measurements of endothelial cell-to-cell and cell-to-substrate gaps and micromechanical properties of endothelial cells during monocyte adhesion. *Proc. Natl Acad. Sci. USA* **99**, 15 638–15 643. (doi:10.1073/pnas.242590799)
33 Guilak, F., Jones, W. R., Ting-Beall, H. P. & Lee, G. M. 1999 The deformation behavior and mechanical properties of chondrocytes in articular cartilage. *Osteoarthritis Cartilage* **7**, 59–70. (doi:10.1053/joca.1998.0162)
34 Rotsch, C., Jacobson, K. & Radmacher, M. 1999 Dimensional and mechanical dynamics of active and stable edges in motile fibroblasts investigated by using atomic force microscopy. *Proc. Natl Acad. Sci. USA* **96**, 921–926. (doi:10.1073/pnas.96.3.921)
35 Darling, E. M., Zauscher, S., Block, J. A. & Guilak, F. 2007 A thin-layer model for viscoelastic, stress-relaxation testing of cells using atomic force microscopy: do cell properties reflect metastatic potential? *Biophys. J.* **92**, 1784–1791. (doi:10.1529/biophysj.106.083097)
36 Oberleithner, H., Peters, W., Kusche-Vihrog, K., Korte, S., Schillers, H., Kliche, K. & Oberleithner, K. 2011 Salt overload damages the glycocalyx sodium barrier of vascular endothelium. *Archiv. Eur. J. Physiol.* **462**, 519–528. (doi:10.1007/s00424-011-0999-1)
37 O'Callaghan, R., Job, K. M., Dull, R. O. & Hlady, V. 2011 Stiffness and heterogeneity of the pulmonary endothelial glycocalyx measured by atomic force microscopy. *Am. J. Physiol. Lung Cell. Mol.* **301**, L353–L360. (doi:10.1152/ajplung.00342.2010)
38 Barker, A. L., Konopatskaya, O., Neal, C. R., Macpherson, J. V., Whatmore, J. L., Winlove, C. P., Unwin, P. R. & Shore, A. C. 2004 Observation and characterisation of the glycocalyx of viable human endothelial cells using confocal laser scanning microscopy. *Phys. Chem. Chem. Phys.* **6**, 1006–1011. (doi:10.1039/b312189e)
39 Megens, R. T. A., Reitsma, S., Schiffers, P. H. M., Hilgers, R. H. P., De Mey, J. G. R., Slaaf, D. W., Oudeegbrink, M. G. A. & Van Zandvoort, M. A. M. J. 2007 Two-photon microscopy of vital murine elastic and muscular arteries: combined structural and functional imaging with subcellular resolution. *J. Vasc. Res.* **44**, 87–98. (doi:10.1159/000098259)
40 Muller, D. J. & Dufrene, Y. F. 2008 Atomic force microscopy as a multifunctional molecular toolbox in nanobiotechnology. *Nat. Nanotechnol.* **3**, 261–269. (doi:10.1038/nnano.2008.100)
41 Hertz, H. 1882 Uber die Beruhrung fester elasticher Korper. *J. für die reine Angew. Math.* **92**, 156–171. (doi:10.1515/crll.1882.92.156)
42 van den Berg, B. M., Vink, H. & Spaan, J. A. E. 2003 The endothelial glycocalyx protects against myocardial edema. *Circ. Res.* **92**, 592–594. (doi:10.1161/01.RES.0000065917.53950.75)
43 Chappell, D., Jacob, M., Paul, O., Rehm, M., Welsch, U., Stoeckelhuber, M., Conzen, P. & Becker, B. F. 2009 The glycocalyx of the human umbilical vein endothelial cell: an impressive structure ex vivo but not in culture. *Circ. Res.* **104**, 1313–1317. (doi:10.1161/CIRCRESAHA.108.187831)
44 Adamson, R. H. & Clough, G. 1992 Plasma proteins modify the endothelial cell glycocalyx of frog mesenteric microvessels. *J. Physiol.* **445**, 473–486.
45 Ebong, E. E., Macaluso, F. P., Spray, D. C. & Tarbell, J. M. 2011 Imaging the endothelial glycocalyx *in vitro* by rapid freezing/freeze substitution transmission electron microscopy. *Arterioscler. Thromb. Vasc. Biol.* **31**, 1908–1915. (doi:10.1161/ATVBAHA.111.225268)